



## Simulation of Convective Heat Transfer and Pressure Drop in Laminar Flow of Al<sub>2</sub>O<sub>3</sub>/water and CuO/water Nanofluids Through Square and Triangular Cross-Sectional Ducts

 S. Zeinali Heris <sup>\*a</sup>, F. Oghazian <sup>b</sup>, M. Khademi <sup>b</sup>, E. saeedi <sup>a</sup>
<sup>a</sup> Department of Chemical Engineering, Ferdowsi University of Mashhad, Mashhad, Iran

<sup>b</sup> Department of Chemical and Petroleum Engineering, Sharif University of Technology, Tehran, Iran

### PAPER INFO

#### Paper history:

Received 03 November 2013

Accepted in revised form 07 October 2014

#### Keywords:

Nanofluid

Convective heat transfer

Dispersion model

Square and triangular cross-sectional ducts

Pressure drop

### ABSTRACT

In this study, the convective heat transfer and pressure drop in laminar flow of Al<sub>2</sub>O<sub>3</sub>/water and CuO/water nanofluids through square and triangular cross-sectional ducts have been numerically investigated using new technique. It has been assumed that there is constant heat flux boundary condition at walls. In addition, to include the presence of nanoparticles, the dispersion model has been used, and the system was solved numerically. Results show that by increasing the volumetric concentration and decreasing the size of nanoparticles, Nusselt number has been enhanced. Also, the Nusselt number increases by increasing the Reynolds number. In all cases, it has been observed that heat transfer coefficient of nanofluid increases in comparison with heat transfer coefficient of pure water. The results show that by adding nanoparticles, pressure drop increases in ducts. In square and triangular ducts, pressure drop is higher when we use CuO/water nanofluid instead of Al<sub>2</sub>O<sub>3</sub>/water nanofluid. In the same way, pressure drop increases by increase of faces of non-circular ducts.

## 1. INTRODUCTION

Nowadays, heat exchangers are of great practical significance in various industrial processes. Due to this importance, many attempts have been made in order to improve the efficiency and to reduce the size of heat exchangers. Generally, larger heat transfer area per volume, greater heat transfer coefficient and lower friction factor are favorable in choosing the duct geometry of heat exchangers (Ray and Misra, 2010). Replacing circular tubes with polygonal ones in shell and tube heat exchangers is one of the alternatives that not only decreases pressure drop in tubes, but also causes a larger surface area per volume which leads to a smaller system size. The triangular duct is the most preferred geometry that offers largest surface area per volume ratio. Square ducts are the next choice, and circular ducts have the least priority. However, in shop fabrication the square and triangular ducts are complicated to install with leak free weld. Also, results of studies on the friction factor of ducts show that in laminar flow, the friction factor in triangular cross-sectional duct is 53.33/Re, while in the rectangular and

circular ones the friction factors are 56.92/Re and 64/Re, respectively. Friction between fluid and inner wall causes losses, which are quantified as pressure drop (Zeinali Heris et al., 2011).

However, the contact area between fluid and exchanger walls in non-circular ducts is less than in circular ones, due to existence of static sections for some parts of fluid near the sharp corners. As a result, heat transfer rate is low because sharp cornered ducts reduce the effective heat transfer surface. A solution for this issue is to use such ducts with rounded corners. Another solution to take the advantages of polygonal ducts and compensating their lower heat transfer rate is to improve thermal properties of fluids. It has been found that adding nanoparticles of specific materials such as metals, oxides and nanotubes can enhance the thermal properties of conventional heat transfer fluids like water, oil and ethylene glycol (Masuda et al., 1993).

Incompact heat exchangers, because of the smaller system dimensions, the hydraulic diameter is small that essentially yields laminar flow in most practical cases. It is therefore necessary to particularly investigate the thermal behavior of ducts in the laminar flow regime.

Many papers have been published on convective heat transfer of nanofluids, and most of them were experimental investigations. However, more studies are

<sup>\*</sup>Corresponding Author's Email: [zeinali@ferdowsi.um.ac.ir](mailto:zeinali@ferdowsi.um.ac.ir) (Z. Heris)

needed to be conducted on numerical investigations of heat transfer in the presence of nanofluids in non-circular ducts (Zeinali Heris et al., 2007a; Choi, 1995; He et al., 2009; Bianco et al., 2010; Izadi et al., 2009).

In general, experimental studies on heat transfer properties of nanofluids emphasize that adding nanoparticles to a base fluid increases convective heat transfer coefficient (Zeinali Heris et al., 2006, 2007b, 2009, 2013, 2014; Sharma et al., 2009; Hwang et al., 2009; Pak and Cho, 1998; Kulkarani et al., 2008; Wen and Ding, 2004; Fotukian and Nasr Esfahani, 2010; Nassan et al., 2010).

Numerical simulations are used to predict heat transfer properties and performance characteristics of nanofluids. Some researchers have already studied the heat transfer properties of nanofluids numerically, but based on our information, a numerical study of pressure drop performance on nanofluids that flows through ducts has been rarely investigated (Salehi et al., 2011).

Xuan and Li (2000) and Xuan and Roetzel (2000) studied nanofluid heat transfer theoretically, and proposed the dispersion model based on chaotic movement of nanoparticles in the main flow. The dispersion model can be applied for describing the heat transfer characteristics of nanofluids (Xuan and Li, 2000). Xuan and Roetzel (2000) proposed a theoretical correlation based on the dispersion model. Khanafar et al. (2003) used this model for modeling of natural convection heat transfer of nanofluids.

Roy et al. (2004) and Maiga et al. (2005) applied a homogeneous model in a radial flow system using numerical investigation of heat transfer of Al<sub>2</sub>O<sub>3</sub>/ethylene glycol and Al<sub>2</sub>O<sub>3</sub>/water nanofluids in a laminar flow; they showed a considerable improvement of heat transfer rates. Zeinali Heris et al. (2011) numerically studied the convective heat transfer of different water based nanofluids flowing through triangular ducts and reported heat transfer improvement. Haghshenas Fard et al. (2010) numerically investigated convective heat transfer of CuO/water nanofluid through a circular tube. They applied CFD (CFX version 11) to model heat transfer in laminar flow and constant wall temperature. They compared the results of two-phase versus single-phase models and reported an increase in heat transfer rate by increasing the concentration of nanoparticles and Peclet number. Askari et al. (2009) numerically studied convective heat transfer with computational fluid dynamic (CFD).

Akbari et al. (2012) carefully examined the CFD predictions of laminar mixed convection of Al<sub>2</sub>O<sub>3</sub>/water nanofluid by single-phase and three different two-phase models (volume of fluid, mixture and Eulerian). In some other papers, heat transfer is investigated with CFD (Hu et al., 2008; Huang et al., 2007). Fereidoon et al. (2013) evaluated the mixed convection in inclined square lid-driven cavity filled with Al<sub>2</sub>O<sub>3</sub>/water nanofluid. The nanofluid flow over

periodic rib-grooved channels in turbulent flow was studied by Vatani and Mohammed (2013).

The convective heat transfer of Al<sub>2</sub>O<sub>3</sub>/water, CuO/water and Cu/water nanofluids through square cross-section duct in a laminar flow with constant temperature boundary conditions is numerically investigated by Zeinali Heris et al. (2012).

Zeinali Heris et al. (2013) experimentally investigated laminar convective heat transfer of Al<sub>2</sub>O<sub>3</sub>/water nanofluid through square cross-sectional. But, in the present work simultaneous effects of the convective heat transfer performance and pressure drop of 2 oxides nanofluid (CuO/water and Al<sub>2</sub>O<sub>3</sub>/water) in laminar flow through square and triangular cross-sectional ducts were numerically studied and compared.

Based on previous studies (Zeinali Heris et al., 2006, 2007b, 2009, 2012, 2013, 2014; Choi, 1995; He et al., 2009; Bianco et al., 2010; Izadi et al., 2009; etc.), most investigated subjects have been the effect of only nanoparticles or different geometries on heat transfer rates. However, in the present study, the effects of type of the nanoparticles (Al<sub>2</sub>O<sub>3</sub>/ CuO) and geometry (Square/Triangular duct) on heat transfer are both investigated simultaneously. In this paper, both square and triangular ducts are chosen to be with the same hydraulic diameter, and the simulation results of adding different nanoparticles and different geometry are studied more comprehensively. Also, the effect of nanoparticles type on pressure drop in ducts studied numerically, and based on the literature this subject is rarely studied.

In this study, the dispersion model and CFD ANSYS Fluent® as the CFD tool, and Gambit as the pre-processor were applied for solving the problem. Gambit generates or imports geometry, and can be used as a basis for simulations in ANSYS Fluent®. For a given geometry, it generates a mesh for the surface and volume of the geometry, allowing it to be used for computational fluid dynamics.

## 2. THEORY

There are different approaches discussed in the literature for investigating heat transfer of nanofluids. In the first approach, nanofluids are considered as two different liquid and solid phases with different momentums. The equations, resulted from two phase theory, are difficult to deal with and cannot be applied easily for nanofluids. In the second approach, both fluid phase and nanoparticles are considered as a homogeneous single phase. Since the particles are ultrafine and become easily fluidized, all the equations of continuity, motion, and energy for pure fluid may directly be extended to nanofluids using thermal and transport properties of nanofluids. Energy equation for nanofluid flow in a rectangular or triangular duct, using

dispersion model, can be written as (Xuan and Li, 2000; Xuan and Roetzel, 2000):

$$\frac{\partial T}{\partial t} + u \frac{\partial T}{\partial x} = \left[ \frac{k_{nf}}{(\rho C_p)_{nf}} + \frac{k_{d,z}}{(\rho C_p)_{nf}} \right] \frac{\partial^2 T}{\partial z^2} + \left[ \frac{k_{nf}}{(\rho C_p)_{nf}} + \frac{k_{d,y}}{(\rho C_p)_{nf}} \right] \frac{\partial^2 T}{\partial y^2} + \left[ \frac{k_{nf}}{(\rho C_p)_{nf}} + \frac{k_{d,x}}{(\rho C_p)_{nf}} \right] \frac{\partial^2 T}{\partial x^2} \quad (1)$$

where terms  $\frac{k_{d,z}}{(\rho C_p)_{nf}}$ ,  $\frac{k_{d,y}}{(\rho C_p)_{nf}}$  and  $\frac{k_{d,x}}{(\rho C_p)_{nf}}$  are added to the energy equation to include the contribution of hydrodynamic dispersion as well as irregular movements of the nanoparticles in the z, y and x directions. The term  $(\rho C_p)_{nf}$  is given by Equation (2) (Xuan and Li, 2000; Xuan and Roetzel, 2000).

$$(\rho C_p)_{nf} = (1 - \varphi)(\rho C_p)_f + \varphi(\rho C_p)_p \quad (2)$$

In this study, the dispersion model, in which the effects of random movements of nanoparticles inside the liquid are considered as excess terms in the heat transfer equation is solved. The effective thermal conductivity of the nanofluid,  $k_{eff}$ , may take the following form (Zeinali Heris et al., 2007a):

$$k_{eff} = k_{nf} + k_d \quad (3)$$

where  $k_d$  is the dispersion thermal conductivity. The structure of nanofluid (dispersed nanoparticles in the base fluid and the interfacial layer of nanoparticles and liquid) is similar to that of porous media. Vadasz (2006) applied a variation of the classical heat conduction method in porous media to solve the problem of heat conduction in nanofluid, and demonstrated that the transient heat conduction process in a nanofluid may provide a valid explanation for the apparent heat transfer enhancement. Using the similarity between a nanofluid and the flow through porous media,  $k_d$  can be expressed as (Drew and Passman, 1999):

$$k_d = C(\rho C_p)_{nf} u_m \varphi D_p a \quad (4)$$

where  $C$  is an unknown constant that can be determined by fitting the results of experimental data. Considering Drew and Passman (1999) the value of  $C$  depends on the diameter of the solid particles and flowing surface geometry. According to the study by Khaled and Vafai (2005) in which heat transfer of nanofluid flow in a channel was investigated, the range of the value of  $C$  was chosen to be from 0 to 0.4. In the present study, compared to Khaled and Vafai's investigation, the values of  $C=0.28$  and  $C=0.3$  are used for rectangular and triangular ducts respectively;  $D_p$  is the diameter of the nanoparticles;  $u_m$  is the average flow velocity;  $\varphi$  is the volume concentration of solid nanoparticles; and  $a$  is the side length of the duct.

The correlation of Yu and Choi (2003) was used for determination of nanofluid effective thermal conductivity as Equation (5):

$$k_{nf} = \left[ \frac{k_s + 2k_w + 2(k_s - k_w)(1 + \beta)^3 \varphi}{k_s + 2k_w - (k_s - k_w)(1 + \beta)^3 \varphi} \right] k_w \quad (5)$$

In Equation (5),  $\beta$  is the ratio of the nanolayer thickness to the original particle radius, and  $\beta=0.1$  was used to calculate the nanofluid effective thermal conductivity (Yu and Choi, 2003).

Physical properties of prepared nanofluids were calculated from water and nanoparticles characteristics at mean inlet and outlet bulk temperature, using following equations for density, viscosity and specific heat (Drew and Passman, 1999):

$$\rho_{nf} = \varphi \cdot \rho_s + (1 - \varphi) \cdot \rho_w \quad (6)$$

$$\mu_{nf} = \mu_w \cdot (1 + 2.5\varphi) \quad (7)$$

Equation (7) is known as Einstein equation (Einstein 1956);  $C_{pnf}$  can be written as:

$$C_{pnf} = \frac{\varphi \cdot (\rho_s \cdot C_{ps}) + (1 - \varphi) \cdot (\rho_w \cdot C_{pw})}{\rho_{nf}} \quad (8)$$

In the study of pressure drop through ducts, the Darcy-Weisbach equation (Shah and London 1978) gives:

$$\Delta p = f \frac{L}{D_H} \frac{\rho_{nf} u_m^2}{2} \quad (9)$$

in which Darcy friction factor relation for triangular and square ducts are  $f = \frac{53.32}{Re}$  and  $f = \frac{56.92}{Re}$ , respectively.

### 3. NUMERICAL SIMULATION

ANSYS Fluent® software was implemented for simulation. The partial differential equations were solved using the finite volume method. ANSYS Fluent® applies a control volume based technique to convert the governing equations into a set of algebraic equations that can be solved numerically. This control volume technique consists of integrating governing equations over each control volume, resulting discrete equations that conserve each quality on a control volume basis.

#### 3.1. Beam and Hybrid Beam-shell Models

In the present study, the length of square and triangular cross-sectional ducts was 1m, and the length of each side was 1cm for square and 1.7cm for triangular ducts. Here, for the purpose of comparing the results, chosen ducts had the same hydraulic diameters. To evaluate the grid sensitivity and to choose the right grid size, wall temperature versus the length of wall for pure water in different grid sizes were examined, and the bigger grid size which did not considerably change the wall temperature of the duct comparing to the smaller size, was selected as the optimal size.

The grid sizes used in the analysis were  $14 \times 14 \times 14 \times 2000$  and  $13 \times 13 \times 2000$  in triangular and square ducts, respectively, which were obtained by dividing each side by 14 parts for triangular duct, and 13 parts for square one, as well as dividing by 2000 parts for the length of the ducts. In order to ensure grid independence, the solution was tested for  $18 \times 18 \times 18 \times 2564$  and  $16 \times 16 \times 2564$

grid sizes for triangular and square ducts, respectively. It was found that decreasing grid sizes from aforementioned values did not lead to significant difference in the wall temperature as it is shown in Figure 1. for Square duct. It should be noticed that the accuracy of simulation is low while bigger grid sizes are chosen; on the other hand, when grid sizes are smaller, the time of solving goes long. In smaller grid sizes after a certain dimension the accuracy would not change considerably and only causes a longer time of solving. Accordingly, those certain sizes are chosen here.

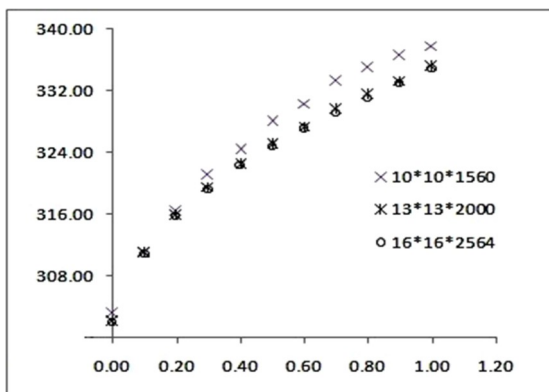


**Figure 1.** Effect of grid size on wall temperature of a square duct in  $Re=2000$

Based on the values of Reynolds numbers that were applied in the simulation (700, 1000, 1300, 1600 and 2000), and calculated physical properties of nanofluids, the related velocities were obtained. The velocity direction was perpendicular to the inlet cross-section of the channel. Inlet temperature of the nanofluid was 295K and the nanofluid was flowing in the  $z$  direction through the duct. Velocity profile was considered to be laminar as well as fully developed, and the duct was long enough, so that the thermally fully developed condition prevailed at the outlet section. Outlet flow condition in ANSYS Fluent<sup>®</sup> software was used as the outlet boundary condition. It was assumed that there was no slip between walls and the fluid. Also, walls of the ducts were kept under the constant heat flux of  $10000\text{w/m}^2$ . Walls were made of copper and had 0.4mm thickness.

**3.2. Validation of computational model** In order to validate the computational model, Figure 2. (a - b) shows the comparison of Nusselt numbers calculated by present simulation and the experimental data obtained from previous published papers on  $\text{Al}_2\text{O}_3/\text{water}$  nanofluid through triangular and square cross sectional duct versus Peclet number Zeinali Heris et al. 2013; 2014). To validate the accuracy of the numerical results obtained by CFD for square cross-sectional duct, the experimental data from (Zeinali Heris et al., 2013) for investigation of 25nm  $\text{Al}_2\text{O}_3/\text{water}$  nanofluid flowing through a square cross-sectional duct was used which is

with the same geometry and conditions of the present study. Figure 2. (a) shows the comparison of the Peclet versus Nusselt number for experimental and CFD data for 25nm  $\text{Al}_2\text{O}_3/\text{water}$  nanofluid in a square cross-sectional duct for 0.5% and 1% of volumetric concentrations.

Comparison of Nusselt numbers resulted from the present simulation and experimental results for 20 nm  $\text{Al}_2\text{O}_3/\text{water}$  nanofluid versus Peclet number in triangular duct (Experimental data from Zeinali Heris et al. 2014) is presented in Figure 2b. As it can be seen, the results of numerical modeling are within the limits of values obtained by experiment. Maximum discrepancy between experimental data and numerical values of the present study is 9%, which verifies the accuracy and reliability of the numerical code.

#### 4. RESULTS AND DISCUSSION

In the present study, the heat transfer characteristics of square and triangular ducts were simulated numerically for  $\text{Al}_2\text{O}_3/\text{water}$  and  $\text{CuO}/\text{water}$  nanofluids in volumetric concentrations of 0.5%, 1%, 1.5% and 2%, and for nanoparticles with diameters of 10, 20, 30 and 40nm at 700, 1000, 1300, 1600 and 2000 Reynolds numbers. The flow regime was laminar and fully developed, and the walls were kept in constant heat flux condition. Every simulation run was performed for a specific Reynolds number, volumetric concentration and nanoparticles size. In total, 160 simulations were run to examine the nanofluids characteristics.

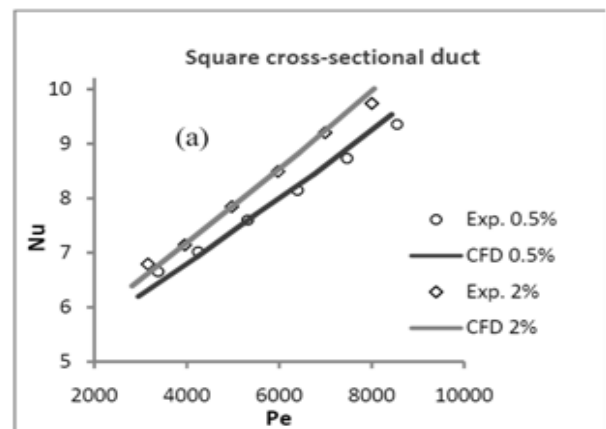


**Figure 2.** (a) Comparison of CFD results and experimental Nusselt number for 25 nm  $\text{Al}_2\text{O}_3/\text{water}$  nanofluid vs. Peclet number for 25 nm  $\text{Al}_2\text{O}_3/\text{water}$  in a square duct. (Experimental data from Zeinali Heris et al., 2013)

In Figure 3. temperature and velocity contours in square and triangular cross-sectional ducts are shown for  $\text{Al}_2\text{O}_3/\text{water}$  nanofluid with 2% volumetric concentration;  $D_p=10\text{nm}$ ; and  $Re=2000$ . The color range from blue to red shows the temperature range from the minimum to the maximum in the duct. As it was expected, formation of hot spots that causes less heat

transfer performance in sharp corners in square and triangular ducts can be seen in this figure. Also, temperature reduces gradually from the walls to the center of the ducts, but the velocity increases from the walls to the center.

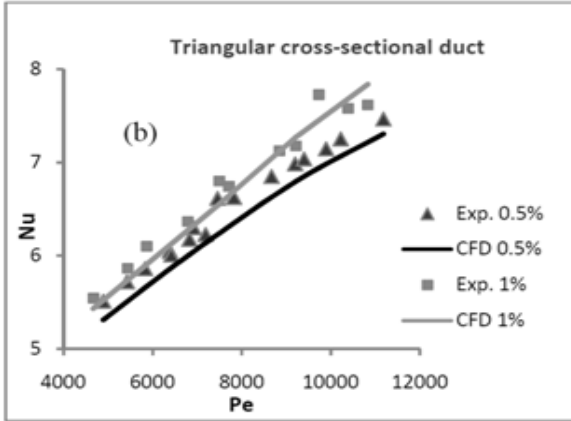


**Figure 2.** (b) Comparison of Nusselt numbers resulted from the present simulation and experimental results for 20 nm  $Al_2O_3$ /water nanofluid versus Peclet number in triangular ducts (Experimental data from Zeinali Heris et al. 2014)

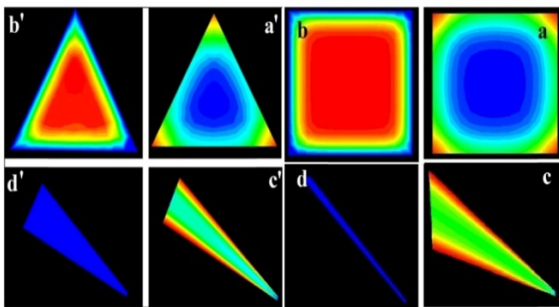


**Figure 3.** Temperature and velocity counters of square and triangular cross-sectional ducts for  $Al_2O_3$ /water nanofluid, V.C=2% ,  $D_p=10nm$ , and  $Re= 2000$ : (a, a') Temperature counters; (b, b') Velocity distribution; (c, c') Temperature distribution at one of the walls of the duct; (d, d') Velocity distribution at one of the walls of the duct

**4. 1. Effect of adding nanoparticles on heat transfer rates**

**4.1.1. Square cross-sectional duct** Nusselt numbers obtained from simulation of  $Al_2O_3$ /water and  $CuO$ /water nanofluids flowing through the square cross-sectional duct, versus Reynolds numbers in different volumetric concentrations and nanoparticle sizes are presented in Figures 4. and 5. As shown in the diagrams of Figure 4. the Nusselt number increases by increase in volumetric concentration, decrease in nanoparticle sizes and increase in Reynolds number.

In all four diagrams, Nusselt numbers of pure water are less than that of  $Al_2O_3$ /water and  $CuO$ /water nanofluid. For example, in Figure 4. for pure water at  $Re=700$ , Nusselt number is 5.43, and for  $Al_2O_3$ /water nanofluid

(V.C.=0.5%,  $Re=700$  and  $D_p=40nm$ ) Nusselt number is 5.53, which shows 1.84% growth. In Figure 4. the Nusselt number has the maximum growth of 48.43% at  $D_p=10 nm$ , V.C.=2% and  $Re=2000$  (in this condition  $Nu=12.78$  while using nanofluid, and  $Nu=8.61$  for pure water). The same conclusions can be drawn for  $CuO$ /water nanofluid from the data which are presented in Figure 5.

In Figures 4. and 5. as size of nanoparticles increases, Nusselt numbers at different volumetric concentrations become approach each other. The maximum difference between Nusselt numbers in different volumetric concentrations can be seen for the particle size of 10nm. On the other hand, the minimum difference between Nusselt numbers is in the diagram that is related to the particle size of 40nm.

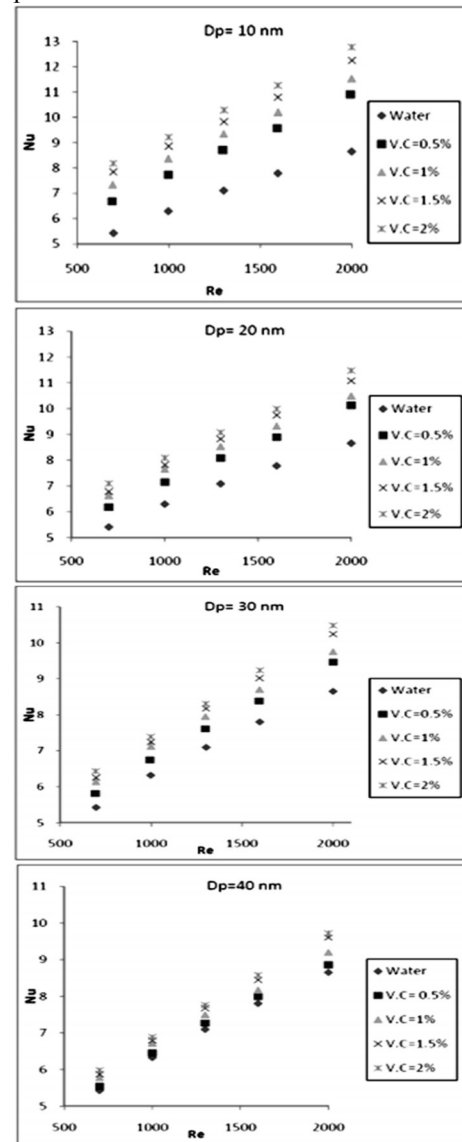


**Figure 4.** Nusselt number versus Reynolds number in different volumetric concentrations and nanoparticle sizes in a square cross-sectional duct for  $Al_2O_3$ /water nanofluid

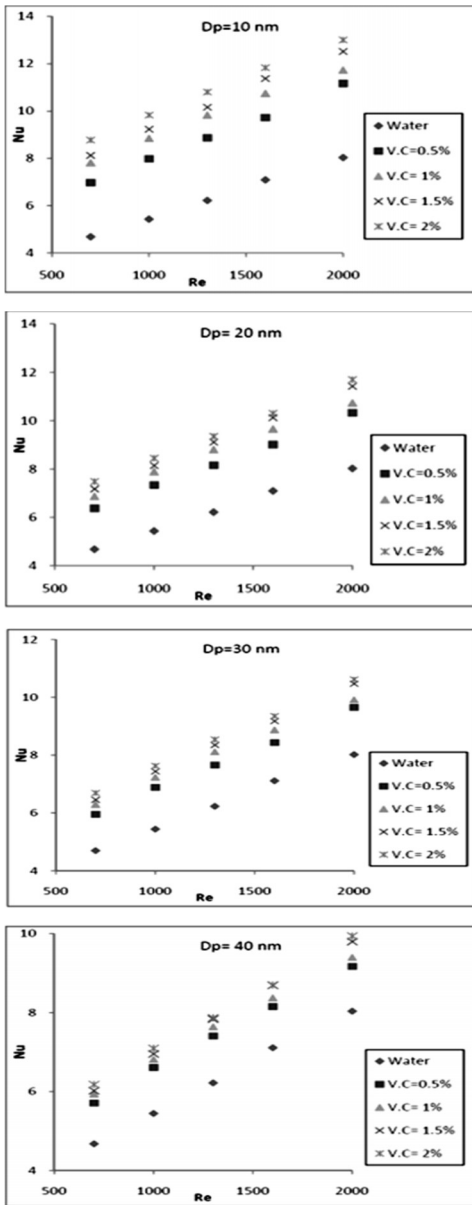


**Figure 5.** Nusselt number versus Reynolds number in different volumetric concentrations and nanoparticle sizes in a square cross-sectional duct for CuO/water nanofluid

**4.1.2. Triangular cross-sectional duct** For a triangular duct with the same hydraulic diameter as the square one ( $D_h = 1\text{cm}$ ) and the same boundary conditions, the diagrams of Nusselt number versus Reynolds number is shown in Figures 6. and 7.

The general results are the same as those for the square duct. In the diagrams of Figure 6. increasing Reynolds numbers from 700 to 2000 in a specific nanoparticle diameter and volumetric concentration leads to increase in Nusselt numbers. Also, in a specific nanoparticle size, by increasing volumetric concentration, Nusselt number increases. For instance, for  $\text{Al}_2\text{O}_3/\text{water}$  nanofluid in  $\text{Re}=2000$  and  $D_p=10\text{nm}$ , by increasing the

volumetric concentration of nanoparticles from 1% to 2%, Nusselt number changes from 10.84 to 12.35.

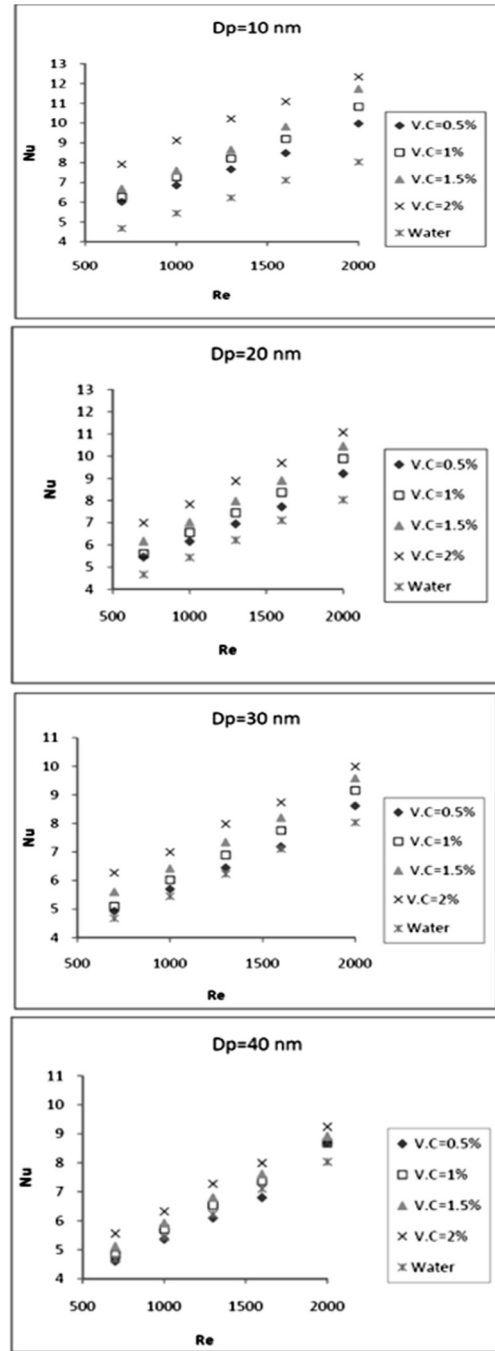


**Figure 6.** Nusselt number versus Reynolds number in different volumetric concentrations and nanoparticle sizes in a triangular cross-sectional duct for  $\text{Al}_2\text{O}_3/\text{water}$  nanofluid

In the same way, Nusselt number increases by increasing nanoparticle sizes in a constant Reynolds number and volumetric concentration. For example, for  $\text{Al}_2\text{O}_3/\text{water}$  in  $\text{Re}=700$ , and  $V.C.=1.5\%$ , the reduction of Nusselt numbers from the particle size of 10nm to 20,

30 and 40nm is 7.77%, 16.29% and 23.47% , respectively.

It can be concluded that enhancing heat transfer rates by means of nanofluids as a heat transfer medium may be used as a trick to overcome the poor heat transfer performance of triangular and square ducts. One possible reason for this heat transfer rate improvement could be the migration of nanoparticles due to shear action, Brownian motion, and viscosity gradient in the cross section of the duct. It seems that presence of nanoparticles may flatten the transverse temperature gradient in the bulk of the fluid (Xuan and Li, 2000), and consequently, enhances convective heat transfer of the nanofluid. In addition, the migration of particles and clustering due to non-uniform shear rate across the duct cross-section, may affect the heat transfer performance.

#### 4.2. Effect of added nanoparticles type on heat transfer

Type of nanoparticles which are added to water to form nanofluid is important for the rate of heat transfer. Conductivity of nanofluids is larger when thermal conductivity of added nanoparticles is high. By comparing diagrams of Figure 4. with Figure 5. and Figure 6. with Figure 7. in square and triangular ducts, the results show that while having the same volumetric concentration, nanoparticle size and Reynolds number, Nusselt number of  $Al_2O_3$ /water nanofluid is smaller than that of CuO/water. Also, by increasing nanoparticle size, Nusselt numbers of the two nanofluids become closer to each other. This effect reveals that in bigger sizes of nanoparticles, the type of added nanoparticle (CuO or  $Al_2O_3$ ) is less important in improvement of heat transfer. In this study, the effect of type of nanoparticle on improvement of heat transfer performance is more important in finer particles (e.g.,  $D_p=10nm$ ), and less while nanoparticles are larger (e.g.,  $D_p=40nm$ ).

In Figure 8. at the same volumetric concentrations, as Reynolds number increases, the difference between Nusselt numbers of two nanofluids decreases with respect to pure water. The maximum difference between Nusselt numbers ratio is at  $Re=700$ , and the minimum difference is at  $Re=2000$ .

It shows that in higher Reynolds, the effect of nanofluid type becomes less important. For example, for  $V.C.=2\%$ , by changing the type of nanofluid in the range of Reynolds numbers of 700, 1000, 1300, 1600 and 2000, the change in the Nusselt numbers ratio is 7.28, 6.84, 5.51, 4.29 and 3.54%, respectively.

Figure 9. shows the effect of added nanoparticles type on Nusselt number in the range of laminar flow Reynolds numbers in a square cross-sectional duct for constant volumetric concentrations of 1% and 2%, and  $D_p=10nm$ .

In this figure, for the same Reynolds numbers and volumetric concentrations, the ratio of Nusselt numbers

of CuO/water nanofluid to pure water is higher than that of  $Al_2O_3$ /water nanofluid to pure water. This indicates that it is more effective to add CuO nanoparticles to water for enhancement of heat transfer rate. For instance, in  $Re=1600$ , and  $V.C.=1\%$ , the ratio of Nusselt number of  $Al_2O_3$ /water to the Nusselt number of pure water is 1.31. By changing nanoparticles to CuO, this ratio increases to 1.36. In  $V.C.=2\%$ , the ratio is 1.42 and 1.49, for  $Al_2O_3$  and CuO nanoparticles, respectively.

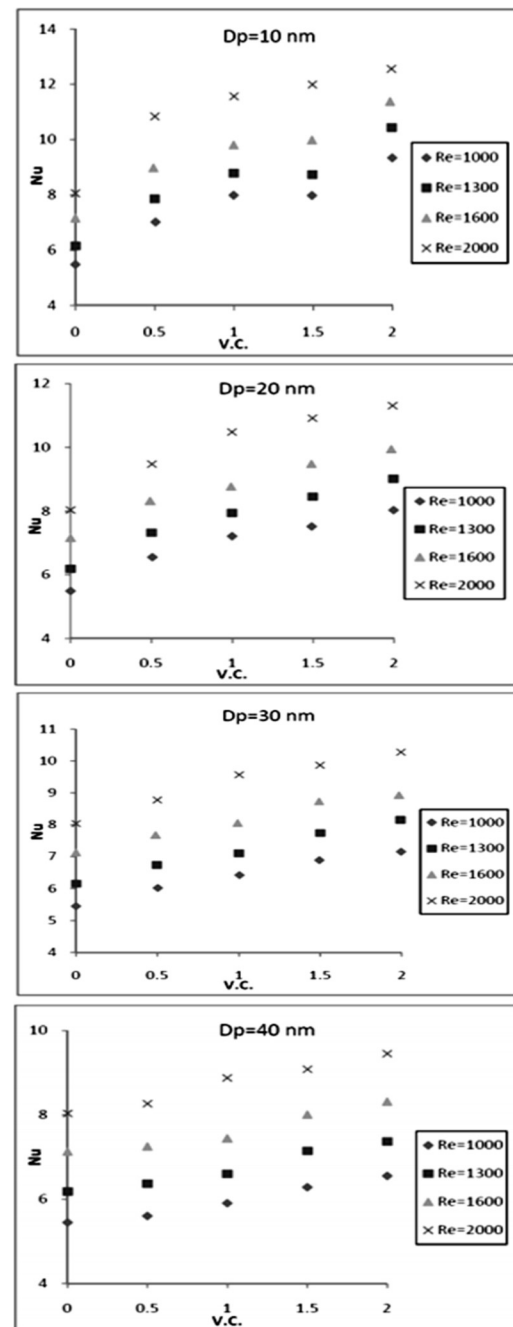


**Figure 7.** Nusselt number versus volumetric concentration in different nanoparticle sizes and Reynolds numbers in a triangular cross-sectional duct for CuO/water nanofluid

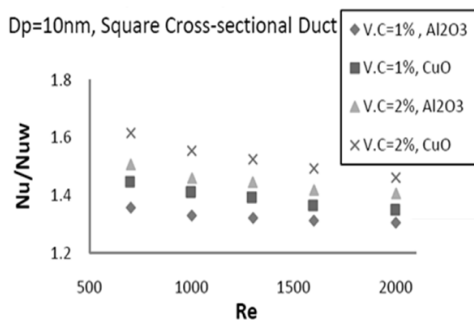


**Figure 8.** Ratio of nanofluids to pure water Nusselt numbers versus Reynolds number in laminar flow in square duct

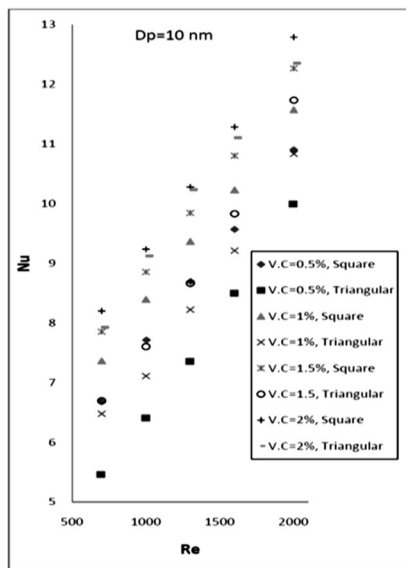


**Figure 9.** Nusselt number versus Reynolds number for  $D_p=10\text{nm}$  and different volumetric concentrations of  $\text{Al}_2\text{O}_3/\text{water}$  nanofluid in square and triangular ducts

#### 4.3. Effect of geometry (Square/triangular cross-sectional ducts) on heat transfer

As mentioned before, the main reason for lower heat transfer rate of the square or triangular duct is the existence of a static section in the vicinity of the duct corners. The presence of nanoparticles causes decrement of these stationary and static sections. One of the possible reasons for heat transfer enhancement may be the migration of nanoparticles to sharp corners of non-circular ducts. Considering the studies on nanofluid heat transfer performance, it can be concluded that adding nanoparticles to the base fluid enhances the heat transfer rate. The enhancement is due to the increment of thermal conductivity, Brownian motion, dispersion, and fluctuation of nanoparticles, particularly near the walls (Zeinali Heris et al., 2006, 2007a; Nassan et al., 2010; Hamed Mousavian et al., 2010).

An increase in the volume fraction of nanoparticles intensifies the interaction and collision of nanoparticles. Moreover, diffusion, migration and relative movement of these particles near the duct walls and corners lead to

mixing and fluctuation of the fluid in these static areas of triangular and square ducts. Subsequently, the decrease of such areas causes rapid heat transfer from the duct walls to the nanofluid.

In Figure 9. Nusselt number versus Reynolds number for nanoparticles of 10nm in size and different volume concentrations of  $\text{Al}_2\text{O}_3/\text{Water}$  nanofluid in square and triangular duct is shown. As can be observed in this figure, Nusselt numbers in square duct are bigger than in triangular one. In the Reynolds numbers of 700, 1000, 1300, 1600 and 2000, Nusselt numbers of square duct are 17.34, 16.44, 9.87, 9.13, and 4.6% bigger than of the triangular one, respectively. As Reynolds number increases, this difference between related Nusselt numbers of two ducts reduces. Therefore, in higher Reynolds numbers, the effects of duct geometry are going to be less important on heat transfer. Same conclusion was drawn for all other sizes of nanoparticles.

#### 4.4. Effect of nanoparticles on pressure drop

##### 4.4.1. Effect of added nanoparticles type on pressure drop

To study the effect of addition of nanoparticles on pressure drop in square and triangular ducts, the results of simulation for pressure drop of  $\text{Al}_2\text{O}_3/\text{water}$  at the minimum volumetric concentration ( $V.C.=0.5\%$ ) are shown in Figure 10. These results show that nanofluids have higher pressure drop comparing to the case that just pure water flows through the duct. For example, in square ducts at  $Re=1600$ , pressure drop while using nanofluid, increases up to 1.06% of that of the state of just using pure water. In triangular ducts, the pressure drop is 1.04% greater than of the case that just pure water flows in the duct. In Figure 10. it can be seen that by increase of Reynolds number, the difference between related pressure drops of pure water and nanofluid increases.

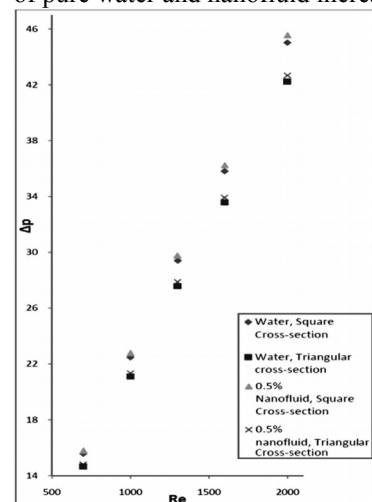


**Figure 10.** Pressure drop (Pa) versus Reynolds in square and triangular ducts for pure water and  $\text{Al}_2\text{O}_3/\text{water}$  nanofluid with the minimum volumetric concentration ( $V.C.=0.5\%$ )



**4.4.2. Effect of nanofluid volumetric concentration on pressure drop** Pressure drop versus Reynolds number at different volumetric concentrations of Al<sub>2</sub>O<sub>3</sub> nanoparticles for square and triangular ducts is shown in diagrams of Figure 11.

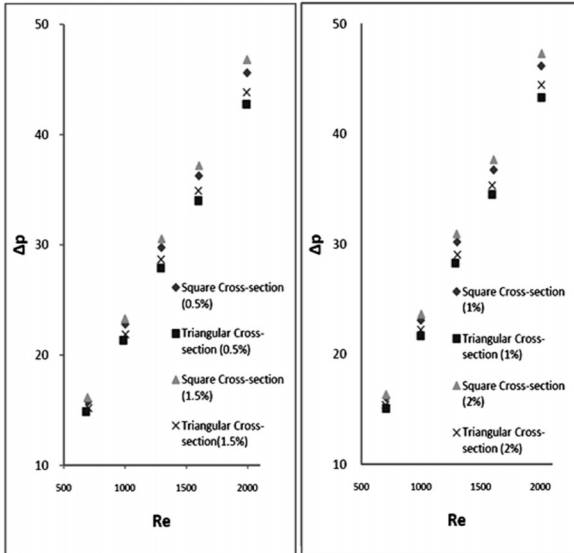


**Figure11.** Pressure drop (Pa) versus Reynolds number for Al<sub>2</sub>O<sub>3</sub>/water nanofluid in square and triangular ducts

As it is demonstrated in this figure, at all Reynolds numbers for laminar flow, by increase of volumetric concentration, pressure drop increases, although not significant. Table 1 indicates how pressure drop changes at Re=2000 by increase of volumetric concentration of Al<sub>2</sub>O<sub>3</sub>/water in a triangular duct. Results show that as volumetric concentration of nanofluid increases, the ratio of nanofluid pressure drop to pure water pressure drop increases. Same conclusions are valid for square duct and CuO/water nanofluid.

**TABLE 1.** Pressure drop for pure water and Al<sub>2</sub>O<sub>3</sub>/water nanofluid in triangular duct at Re=2000

V.C.	2%	1.5%	1%	0.5%	Pure water
Pressure drop (Pa)	46.63	45.5	44.37	43.24	42.23
Pressure drop of nanofluid/Pressure drop of pure water	1.1	1.08	1.05	1.02	1

**4.4.3. The effect of velocity and fluid flow rate on pressure drop** The changes in Reynolds numbers in laminar flow through the duct result from changes in inlet flow rate or fluid velocity. Diagrams of Pressure drop versus volumetric concentration for different Reynolds numbers in square and triangular cross-sectional ducts for Al<sub>2</sub>O<sub>3</sub>/water and CuO/water nanofluids are shown in Figure 12. From this figure, it can be concluded that pressure drop increases by increase of Reynolds number.

**4.4.4. The effect of added nanoparticles type to the base fluid on pressure drop in the duct**

To show the effects of nanoparticles on the shear stress in the duct, the pressure drop of Al<sub>2</sub>O<sub>3</sub>/water and CuO/water nanofluids flowing through triangular and square ducts, for two different Reynolds numbers, versus volumetric concentration is shown in Figure 13. As it is shown, the type of added nanoparticles has different effects on pressure drop in the ducts. In a specific duct, for the same Reynolds number and volumetric concentration, pressure drop for CuO/water is higher than of Al<sub>2</sub>O<sub>3</sub>/water nanofluid. For example, when the Al<sub>2</sub>O<sub>3</sub>/water nanofluid flows in the square duct with Re=2000 and V.C.=2%, pressure drop is 47.39Pa. In the same conditions, pressure drop for CuO/water nanofluid is 49.78Pa(5.04% greater than of Al<sub>2</sub>O<sub>3</sub>/water nanofluid). For the triangular duct with Re=1600 and V.C.=1.5%, the pressure drop is 34.86 and 36.20 for Al<sub>2</sub>O<sub>3</sub>/water and CuO/water nanofluids, respectively, that indicates higher pressure drop for CuO/water nanofluid. The same trend can be observed for other Reynolds numbers and volumetric concentrations.

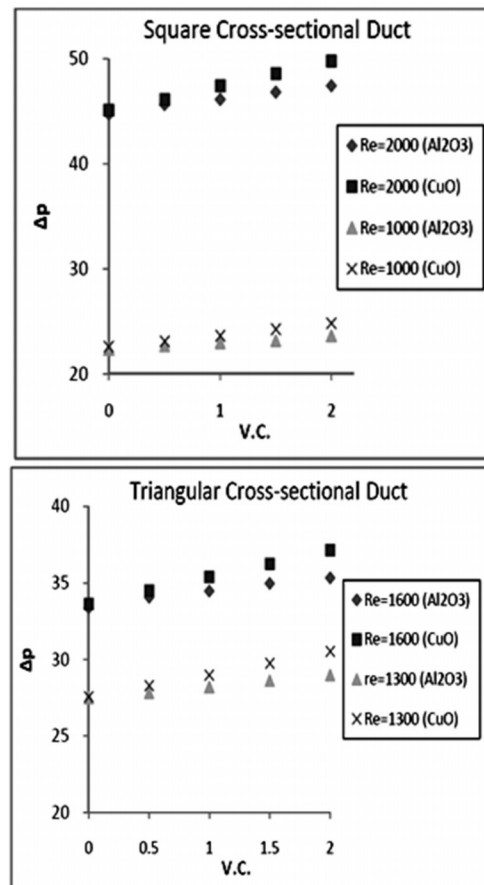


**Figure13.** Pressure drop (Pa) versus volumetric concentration in square and triangular ducts

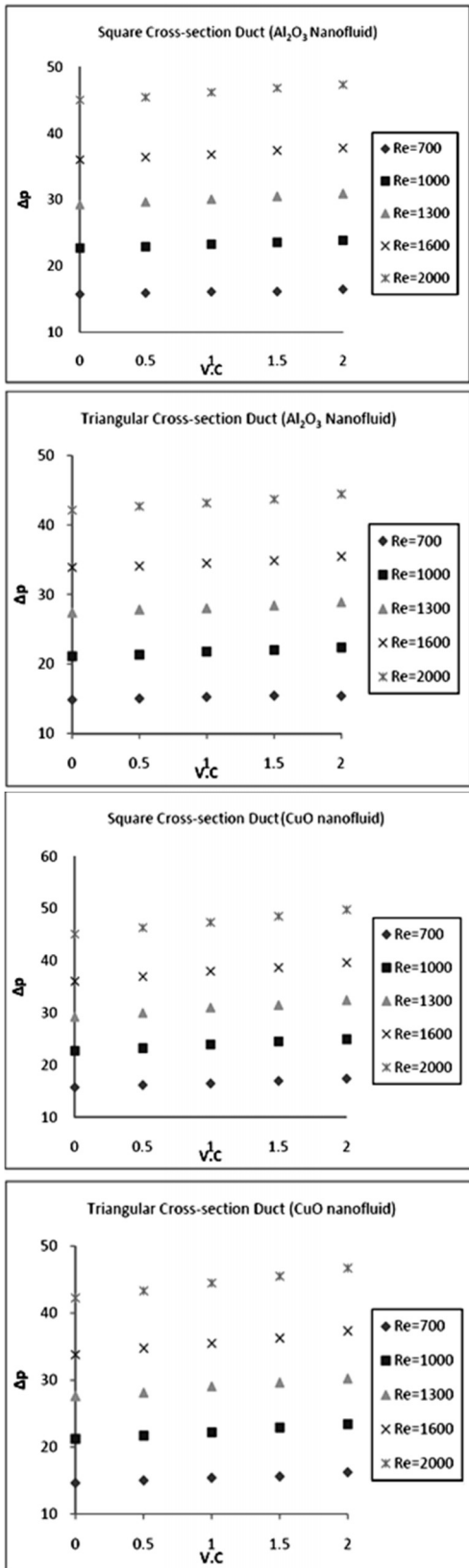


Figure12. Pressure drop versus volumetric concentration for Al<sub>2</sub>O<sub>3</sub>/water and CuO/water nanofluids in different Reynolds numbers for triangular and square ducts

**4.4.5. The effect of geometry on pressure drop in ducts**

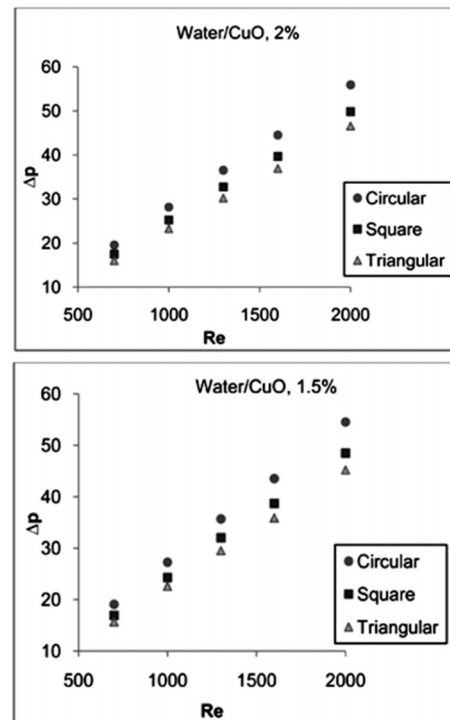
The results of this study show that in polygonal ducts, by increase in faces of the ducts, pressure drop increases. In Figure 14. pressure drop versus Reynolds number for triangular, square and circular ducts at different volumetric concentrations of CuO/water nanofluid, is plotted. It can be seen that for all Reynolds numbers and volumetric concentrations, the pressure drop in circular duct is the highest. Also, the effect of duct geometry is more significant at higher Reynolds numbers.

**4.5. Evaluation of Performance Index**

As it was mentioned before, adding nanoparticles to the water increases the heat transfer rate. Besides, the pressure drop caused by addition of nanoparticles must be reasonable and efficient, so a third factor must be considered with respect to the pressure drop and heat transfer coefficient. This factor is defined as performance index ( $\epsilon$ ) and is evaluated by the following equation (Anoop et al. 2009):

$$\epsilon = \frac{\frac{h_{nf}}{h_{base\ fluid}}}{\frac{\Delta p_{nf}}{\Delta p_{base\ fluid}}} \tag{10}$$

where  $h_{nf}$  and  $h_{base\ fluid}$  are the heat transfer coefficients of the nanofluids and base pure water, respectively;  $\Delta p_{nf}$  and  $\Delta p_{base\ fluid}$  are the pressure drops of the nanofluids and the base pure water, respectively. Based on Equation (11), at performance indexes of greater than 1, using nanofluids to improve the heat transfer performance, is quite applicable.



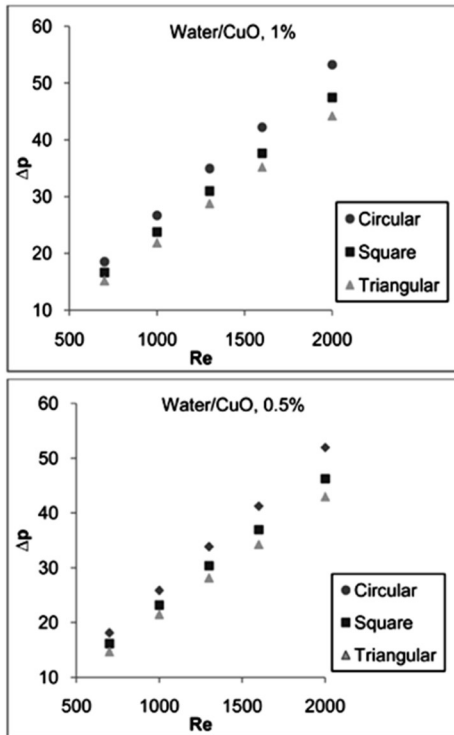


**Figure14.** Pressure drop versus Reynolds number for different volumetric concentration of CuO/water nanofluid

In Figure 15, the performance indexes of CuO/water and Al<sub>2</sub>O<sub>3</sub>/water nanofluids are shown versus Reynolds number at different volumetric concentrations and nanoparticle sizes for triangular and square cross-sectional ducts.

According to Figure 15, the related performance indexes of nanofluids for all conditions are greater than 1, which reveals that in all runs, heat transfer rate was improved by adding nanoparticles to the base fluid. The minimum performance index was 1.31, for the case of using Al<sub>2</sub>O<sub>3</sub>/water nanofluid flowing in the triangular cross-sectional ducts with the volumetric concentration of 0.5%, Re=1600, and Dp=40nm.

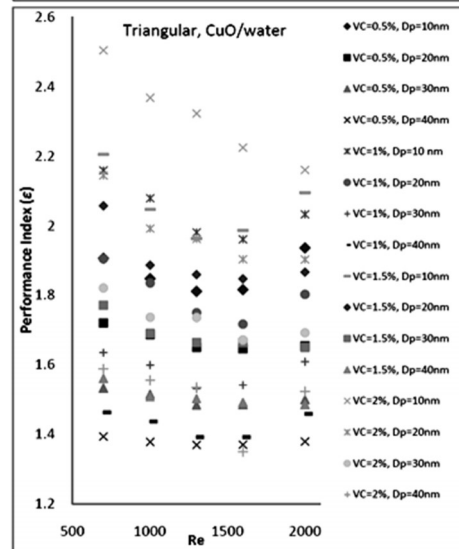
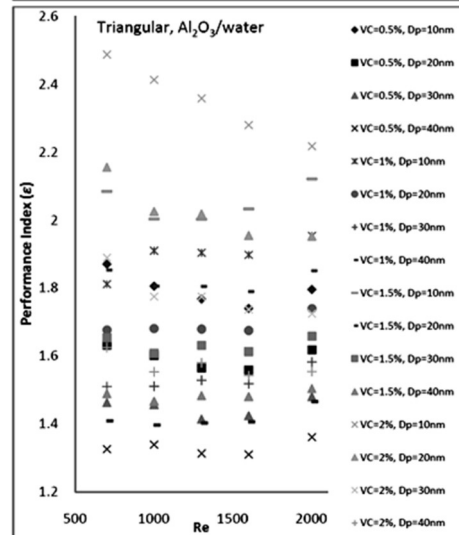
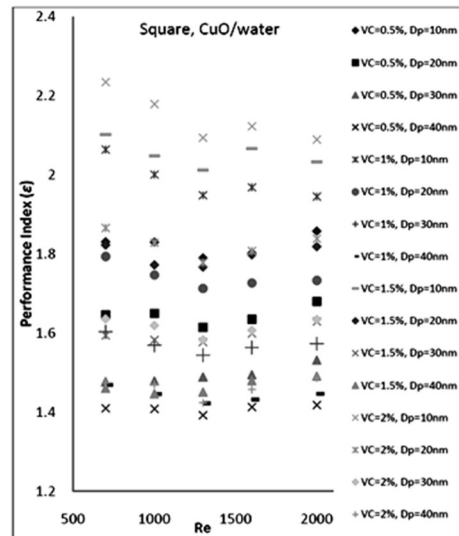
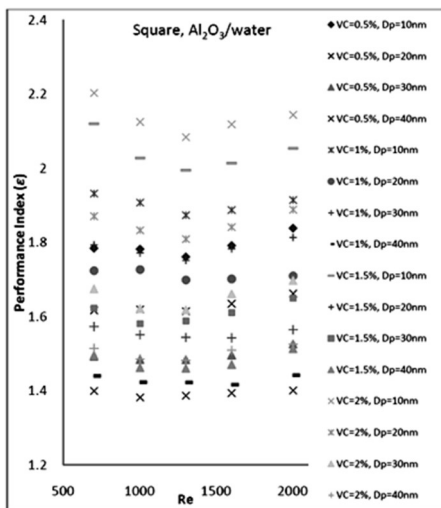


**Figure15.** Performance Index of Al<sub>2</sub>O<sub>3</sub>/water and CuO/Water nanofluids versus Reynolds number at different volumetric concentrations and nanoparticle sizes for triangular and square cross-sectional ducts

## 5. CONCLUSION

Laminar, fully developed, convective heat transfer of Al<sub>2</sub>O<sub>3</sub>/water and CuO/water nanofluids flowing through triangular and square ducts with constant heat flux boundary condition was numerically studied in this article. The results show that adding of nanoparticles to the base fluid, causes remarkable increase in heat transfer coefficients, compared to the base pure water. Heat transfer enhances by increase of nanoparticle concentration in the fluid.

Also, the results of the numerical solution showed that increase in nanoparticle size leads to decrease in Nusselt number. Studying the effect of duct geometry on nanofluids heat transfer rates indicated that the Nusselt number of the square duct is higher than that of the triangular one (at the same Reynolds number, volumetric concentration and nanoparticle size). At a specific Reynolds number, in square and triangular ducts using CuO/water nanofluid, Nusselt number is greater than that of using Al<sub>2</sub>O<sub>3</sub>/water nanofluid.

In addition, the effect of adding nanoparticles on pressure drop was investigated, and it was concluded that by adding nanoparticles, pressure drop in the ducts increases. Also, as volumetric concentration of nanofluid increases, pressure drop through ducts increases as well. In square and triangular ducts, pressure drop is higher when using CuO/water nanofluid instead of Al<sub>2</sub>O<sub>3</sub>/water nanofluid. In the same way, pressure drop increases by changing the duct geometry from triangular to square, and from square to circular ducts. In fact, pressure drop increases by increase of faces of non-circular ducts.

Since the main purpose of adding nanoparticles to the base water is increasing the heat transfer rate, a third parameter defined as performance index ( $\epsilon$ ) is introduced to show the heat transfer improvement. At performance indexes of greater than 1, using nanofluids is quite applicable. The performance indexes of the nanofluids for all the runs were greater than 1 which reveals that all the runs are practically useful.

## Nomenclature

$a$	side length of square duct, m
$b$	side length of triangular duct, m
$C_p$	specific heat, kJ/kg.K
$D_p$	diameter of nanoparticles, nm
$D_h$	Hydraulic diameter, m
$h$	Convective Heat Transfer Coefficient, W/m <sup>2</sup> .K
$k$	Thermal Conductivity, W/m.K
$L$	Length of the duct, m
$Nu$	Nusselt Number
$q$	Heat Flux, W/m <sup>2</sup>
$Re$	Reynolds Number
$t$	Time, s
$T$	Fluid temperature, K
$u$	Velocity of fluid, m/s
$V$	Volume, m <sup>3</sup>

## Subscripts

$d$	dispersed
$eff$	effective
$f$	fluid
$max$	maximum
$nf$	nanofluid
$w$	water

## Greek letters

$\mu$	Viscosity, Pa.s
$\phi$	Nanoparticles volume concentration ( $V.C.$ )
$\rho$	Density, kg.m <sup>-3</sup>

## 6. ACKNOWLEDGMENT

The authors would like to thank Nano Research Center of Iran for financially support of this project.

## REFERENCES

1. Akbari, M., Galanis, N. and Behzadmehr, A., "Comparative analysis of single and two-phase models for CFD studies of nanofluid heat transfer", *International Journal of Thermal Sciences*, Vol. 50, No. 8, (2012), 1343-1354.
2. Anoop, K.B., Sundararajan, T. and Das, S.K., "Effect of Particle Size on the Convective Heat Transfer in Nanofluid in the Developing Region", *International Journal of Heat and Mass Transfer*, Vol. 52, (2009), 2189-2195.
3. Askari, B., Gandjalikhan Nassab, S.A. and Peymanfard, M., "Numerical analysis of convective heat transfer in supercritical water flow channels", *Engineering Applications of Computational Fluid Mechanics*, Vol. 3, No. 3, (2009), 408-418.
4. Bianco, V., Manca, O. and Nardini, S., "Numerical simulation of water/Al<sub>2</sub>O<sub>3</sub> Nanofluid turbulent convection", *Advances Mechanical Engineering*, Vol. 2010, (2010), 1-10.
5. Choi, S.U.S., "Enhancing thermal conductivity of fluids with nanoparticles", *Developments and applications of non-Newtonian flows American Society of Mechanic Engineers*, Vol. FED 231, (1995), 99-105.
6. Drew, D.A. and Passman, S.L., "Theory of Multi Component Fluids", Applied Mathematical Sciences, Berlin, Springer, (1999).
7. Einstein, A., "Investigation on Theory of Brownian motion", New York, Dover, (1956).
8. Fereidoon, A., Saedodin, S., Hemmat Efe, M. and Noroozi, M.J., "Evaluation of Mixed Convection in Inclined Square Liddriven Cavity Filled with Al<sub>2</sub>O<sub>3</sub>/Water Nano-Fluid", *Engineering Applications of Computational Fluid Mechanics*, Vol. 7, No. 1, (2013), 55-65.
9. Fotukian, S. M. and Nasr Esfahany, M., "Experimental study of turbulent convective heat transfer and pressure drop of dilute CuO/ water Nanofluid inside a circular tube", *International Communications in Heat and Mass Transfer*, Vol. 37, No. 2, (2010), 214-219.
10. Haghshenas Fard, M., Nasr Esfahany, M. and Talaie, M.R., "Numerical study of convective heat transfer of nanofluids in a circular tube two-phase model versus single-phase model", *International Communications in Heat and Mass Transfer*, Vol. 37, No. 1, (2010), 91-97
11. Hamed Mosavian, M.T., Zeinali Heris, S., Etemad, S.Gh. and Nasr Esfahany M., "Heat transfer enhancement by application of nano-powder", *Journal of Nanoparticle Research*, Vol. 12, No. 7, (2010), 2611-2619.

12. He, Y., Men Y., Zhao, Y., Lu, H. and Ding, Y., "Numerical investigation into the convective heat transfer of TiO<sub>2</sub> nanofluids flowing through a straight tube under the laminar flow conditions", *Applied Thermal Engineering*, Vol. 29, No. 10, (2009), 1965-1972.
13. Hu, S., Seo, Y., McFarland, AR. and Haglund, J.S., "Heat transfer study on a bioaerosol sampling cyclone", *Engineering Applications of Computational Fluid Mechanics*, Vol. 2, No. 3, (2008), 309-318.
14. Huang, H. and Fang, Y., "MHD effect on heat transfer in liquid metal free surface flow around a cylinder", *Engineering Applications of Computational Fluid Mechanics*, Vol. 1, No. 2, (2007), 88- 95.
15. Hwang, K. S., Jang, S.P. and Choi, S.U.S., "Flow and convective heat transfer characteristics of water-based Al<sub>2</sub>O<sub>3</sub> nanofluids in fully developed laminar flow regime", *International Journal of Heat and Mass Transfer*, Vol. 52, (2009), 193-199.
16. Izadi, M., Behzadmehr, A. and Jalali-Vahida, D., "Numerical study of developing laminar forced convection of a nanofluid in an annulus", *International Journal of Thermal Sciences*, Vol. 48, No.11, (2009), 2119-2129.
17. Khaled, A-RA. and Vafai, K., "Heat transfer enhancement through control of thermal dispersion effects", *International Journal of Heat and Mass Transfer*, Vol. 48, (2005), 2172-2185
18. Khanafer, K., Vafai, K. and Lightstone, M., "Buoyancy-driven heat transfer enhancement in a two-dimensional enclosure utilizing Nanofluids", *International Journal of Heat and Mass Transfer*, Vol. 46, No. 19, (2003), 3639 -3653.
19. Kulkarni, D. P., Namburu, P.K., Bargar, H.E. and Das, D.K., "Convective heat transfer and fluid dynamic characteristics of SiO<sub>2</sub> ethylene glycol/water Nanofluid", *Heat Transfer Engineering*, Vol. 29, No. 12, (2008), 1027-1035.
20. Maïga, S.E.B., Palm, S.J., Nguyen, C.T., Roy, G. and Galanis, N., "Heat transfer enhancement by using nanofluids in forced convection flows", *International Journal of Heat and Fluid Flow*, Vol. 26, No. 4, (2005), 530 -546.
21. Masuda, H., Ebata, A., Teramat, K. and Hishinuma, N., "Alteration of Thermal Conductivity and Viscosity of Liquid by Dispersing Ultra-fine Particles (Dispersion of c-Al<sub>2</sub>O<sub>3</sub>, SiO<sub>2</sub> and TiO<sub>2</sub> Ultra-fine particles)", *Netsu Bussei (Japan)*, Vol. 7, No. 4, (1993), 227-233.
22. Nassan, T.H., Zeinali Heris, S. and Noie, S.H., "A comparison of experimental heat transfer characteristics for Al<sub>2</sub>O<sub>3</sub>/water and CuO/water nanofluids in square cross-section duct", *International Communications in Heat and Mass Transfer*, Vol. 37, No. 7, (2010), 924-928.
23. Pak, B.C. and Cho, Y.I., "Hydrodynamic and heat transfer study of dispersed fluids with submicron metallic oxide particles", *Experimental Heat Transfer*, Vol. 11, No. 2, (1998), 151-170.
24. Ray, S. and Misra, D., "Laminar fully developed flow through square and equilateral triangular ducts with rounded corners subjected to H1 and H2 boundary conditions", *International Journal of Thermal Sciences*, Vol. 49, (2010), 1763-1775.
25. Roy, G., Nguyen C.T. and Lajoie, P., "Numerical investigation of laminar flow and heat transfer in a radial flow cooling system with the use of nanofluids", *Superlattices and Microstructures*, Vol. 35, (2004), 497-511.
26. Salehi, H., Zeinali Heris, S., Koolivand Salooki, M. and Noei, S.H., "Designing a neural network for thermosyphon with nanofluid using a genetic algorithm", *Brazilian Journal of Chemical Engineering*, Vol. 28, No. 1, (2011), 157-168.
27. Shah, R.K. and London, A.L. Laminar flow forced convection in ducts: a source book for compact heat exchanger analytical data, New York, Academic Press, (1978).
28. Sharma, K.V., Sunder, L.S. and Sarma, P.K., "Estimation of heat transfer coefficient and friction factor in the transition flow with low volume concentration of Al<sub>2</sub>O<sub>3</sub> nanofluid flowing in a circular tube and with twisted tape insert", *International Communications in Heat and Mass Transfer*, Vol. 36, No. 5, (2009), 503-507.
29. Sieder, E. N. and Tate, G.E., "Heat transfer and pressure drop of liquid in tubes", *Industrial & Engineering Chemistry*, Vol. 28, No. 12, (1936), 1429-1435.
30. Vadasz, P., "Heat conduction in nanofluid suspensions", *Journal of Heat Transfer*, Vol. 128, No. 5, (2006), 465-477.
31. Vatani, A. and Mohammed, H.A., "Turbulent nanofluid flow over periodic rib-grooved channels", *Engineering applications of Computational Fluid Mechanics*, Vol. 7, No. 3, (2013), 369-381.
32. Wen, D. and Ding, Y., "Experimental investigation into convective heat transfer of nanofluids at the entrance region under laminar flow conditions", *International Journal of Heat and Mass Transfer*, Vol. 47, No. 24, (2004), 5181-5188.
33. Xuan, Y. and Li, Q., "Heat transfer enhancement of nanofluids", *International Journal of Heat and Fluid Flow*, Vol. 21, No. 1, (2000), 58-64.
34. Xuan, Y. and Roetzel, W., "Conceptions for heat transfer correlation of nanofluid", *International Journal of Heat and Mass Transfer*, Vol. 43, No. 19, (2000), 3701-3707.
35. Yu, W. and Choi, S.U.S., "The role of interfacial layers in the enhanced thermal conductivity of nanofluids: a renovated Maxwell model", *Journal of Nanoparticle Research*, Vol. 5 No. (1-2), (2003), 167-171.
36. Zeinali Heris, S., Etemad, S.Gh. and Nasr Esfahany, M., "Convective heat transfer of a Cu/water nanofluid flowing through a circular tube", *Experimental Heat Transfer*, Vol. 22, No. 4, (2009), 217-227.
37. Zeinali Heris, S., Kazemi-Beydokhti, A., Noie, S.H. and Rezvan, S., "Numerical study on convective heat transfer of Al<sub>2</sub>O<sub>3</sub>/water, CuO/water and Cu/water nanofluids through square cross-section duct in laminar flow", *Engineering Applications of Computational Fluid Mechanics*, Vol. 6, No. 1, (2012), 1- 14.
38. Zeinali Heris, S., Nasr Esfahany, M. and Etemad, S.Gh., "Investigation of CuO/water nanofluid Laminar convective heat transfer through a circular tube", *Journal of Enhanced Heat Transfer*, Vol. 13, No. 4, (2006), 279-289.
39. Zeinali Heris, S., Nasr Esfahani, M. and Etemad, S.Gh., "Numerical investigation of nanofluid laminar convective heat transfer through a circular tube", *Numerical Heat Transfer Part A*, Vol. 52, No. 11, (2007), 1043-1058.
40. Zeinali Heris, S., Nasr Esfahany, M. and Etemad, S. Gh., "Experimental investigation of convective heat transfer of Al<sub>2</sub>O<sub>3</sub>/water nanofluid in circular tube", *International Journal of Heat and Fluid Flow*, Vol. 28, No. 2, (2007), 203-210.
41. Zeinali Heris, S., Nassan, T.H. and Noie, S.H., "CuO/Water nanofluid convective heat transfer through square duct under uniform heat flux", *International Journal Nanoscience and Nanotechnology*, Vol. 7, No. 3, (2011), 111-120.
42. Zeinali Heris, S., Noie, S.H., Talaii, E. and Sargolzaei, J., "Numerical investigation of Al<sub>2</sub>O<sub>3</sub>/water nanofluid laminar convective heat transfer through triangular ducts", *Nanoscale Research Letters*, Vol. 6, (2011), 179-189.
43. Zeinali Heris, S., Nassan, T.H., Noie, S.H., Sardarabadi, H. and Sardarabadi, M., "Laminar convective heat transfer of Al<sub>2</sub>O<sub>3</sub>/water nanofluid through square cross-sectional duct", *International Journal of Heat and Fluid Flow*, Vol. 44, (2013), 375-382.
44. Zeinali Heris, S., Edalati Z., Noie, S.H. and Mahian, O., "Experimental investigation of Al<sub>2</sub>O<sub>3</sub>/water nanofluid through equilateral triangular duct with constant wall heat flux in laminar flow", *Heat Transfer Engineering*, Vol. 35, No. 13, (2014), 1173-1182.